Acoustic phonon-assisted resonant tunneling via single impurities

M. Gryglas,[1] M. Baj,[1] B. Chenaud,[2] B. Jouault,[2] A. Cavanna,[3] and G. Faini[3]
[1]*Institute of Experimental Physics, Warsaw University, Poland*
[2]*Groupe d'Étude des Semiconducteurs, Université Montpellier II, Montpellier, France*
[3]*Laboratoire de Photonique et de Nanostructures, Marcoussis, France*
(Received 20 October 2003; published 5 April 2004)

We perform the investigations of the resonant tunneling via impurities embedded in the AlAs barrier of a single GaAs/AlGaAs heterostructure. In the $I(V)$ characteristics measured at 30 mK, the contribution of individual donors is resolved and the fingerprints of phonon assistance in the tunneling process are seen. The latter is confirmed by detailed analysis of the tunneling rates and the modeling of the resonant tunneling contribution to the current. Moreover, fluctuations of the local structure of the DOS (LDOS) and Fermi edge singularities are observed.

DOI: 10.1103/PhysRevB.69.165302 PACS number(s): 73.23.Hk, 73.20.Hb, 72.10.Di

I. INTRODUCTION

A considerable amount of resonant tunneling studies was performed on single barrier GaAs/AlAs/GaAs heterostructures. AlAs is an indirect gap material with the minimum of the conduction band at the X point of the Brillouin zone, while in GaAs the minimum is at the Γ point. As one can see in Fig. 1, the bands are aligned in a way that AlAs layer forms a barrier for the electrons in the Γ valley (solid line), and a quantum well (QW) for the X valley electrons (dashed line). There were several analyses of tunneling through X-valley states including first observation of negative differential resistance in such structures,[1] considerations of Γ-X transfer mechanisms,[2] discussion of momentum conservation,[3] as well as through X-minimum-related donor states (including investigations of the splitting of the ground state,[4,5] pressure coefficients,[6] and binding energies[7] of donors). However, in those experiments macroscopic samples were used where many donors were involved. Recently, interest was more focussed on the observation of the tunneling through individual objects such as quantum dots or impurities. In this case it is possible to perform the spectroscopy of the two-dimensional electron gas (2DEG) in the so-called emitter[8] as well as of these individual objects which are involved in the tunneling, e.g., quantum dots.[9]

In this paper we report results of resonant tunneling experiments performed on GaAs/AlAs/GaAs single barrier junctions in which single impurities, incorporated in the AlAs layer, are involved. Some additional features (like Fermi edge singularity and fluctuations of the LDOS) are also discussed.

II. SAMPLE FABRICATION

Samples were grown by molecular beam epitaxy on a (100)-oriented Si-doped n-type GaAs wafer ($n_d = 1 \times 10^{18}$ cm^{-3}). The active part of the heterostructure consists of a 10.2 nm thick AlAs barrier incorporating a Si δ doping in the middle with a concentration of $n_\delta = 1 \times 10^{10}$ cm^{-2}. In some reference samples the Si δ doping is omitted. The barrier is separated from the heavily doped contacts ($n_d = 4 \times 10^{18}$ cm^{-3}) by 200 nm GaAs spacers in order to obtain high quality 2DEG. Mesa structures of different lateral sizes ranging from 500 μm down to 100 nm were fabricated. This allows us to have different numbers of donors within the junction, starting from more than 10^6 for the larger mesas to less than 10 for the smallest ones.

III. EXPERIMENTAL RESULTS FOR LARGE MESAS

Figure 2 shows current versus voltage characteristics measured at 4.2 K on 500 μm mesas, one δ-doped (10^{10} cm^{-2}, solid line), the other one undoped (dashed line). In the $I(V)$ curve of the doped mesa we observe an important increase of the tunneling current at approximately 1 V. This is related to the resonant tunneling through donor states,[4] and since in this case the number of donors is huge (5×10^6), the observed increase is very broad. The other current bump at about 2 V, present for both samples, is due to the tunneling through X-minimum quantum well states.[4,6]

IV. EXPERIMENTAL RESULTS FOR SMALL MESAS

If the number of Si impurities inside the barrier decreases[10] (small mesas), then the contribution of one individual Si impurity can be resolved.[11] In Fig. 3 we present the $I(V)$ characteristic of a 400 nm mesa, measured at very low temperature (30 mK). The diameter is so small that the ex-

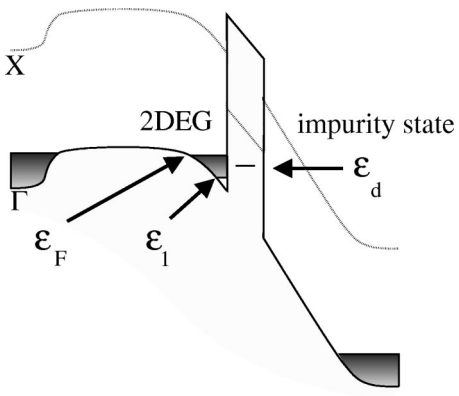

FIG. 1. Sketch of the conduction band under applied bias. Solid line: Γ valley, dotted line: X valley.

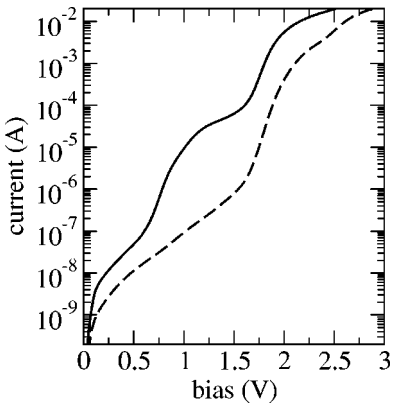

FIG. 2. $I(V)$ curves for large (0.5 mm wide) doped (solid) and undoped (dashed) mesas.

pected average number of donors within the mesa is of the order of 10.

We observe several sharp current increases (labeled for clarity), which are followed either by the decrease of tunneling current (e.g., 1,3) or by further current increases (2,4). The observed features can be qualitatively explained in the following way: each of the increases indicates the beginning of the resonant tunneling process via an impurity level, whose energy (ϵ_d) becomes aligned with the Fermi energy (ϵ_F) in the emitter. Then, as the voltage increases further, the impurity level goes down with respect to ϵ_F but remains aligned with occupied states in the emitter, so that the tunneling current is maintained. Once it is below the bottom of the subband in the emitter, the current decreases.

The fact that we observe many steps spread in a relatively wide bias range indicates that some interdiffusion of Si atoms takes place during the growth and the Si δ layer is broadened. The steps which appear at low biases correspond to donors placed close to the collector side of AlAs layer. In electric field, the position at which the binding energy of the impurity has its maximum is shifted from the center of the AlAs layer[12,13] to the collector side of the structure.[14]

The above considerations lead to the conclusion that one

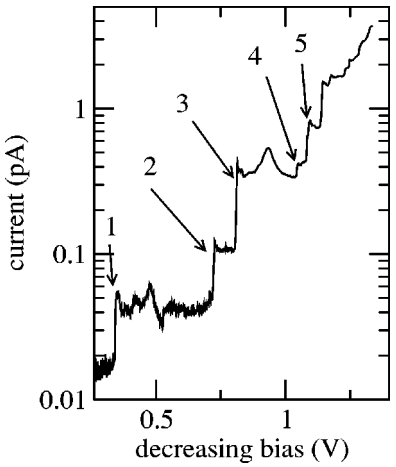

FIG. 3. $I(V)$ curve for a 400 nm mesa measured at very low temperature (30 mK).

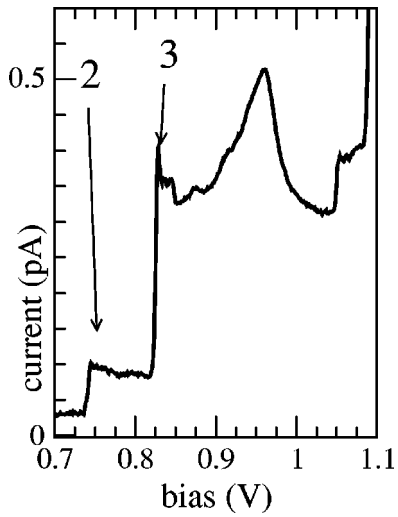

FIG. 4. Detailed measurement of step 3 from Fig. 3.

should expect a rectangular shape in $I(V)$ characteristics while measuring the tunneling from 2DEG through a localized state at very low T. However, a more complex structure is systematically observed. Let us discuss this point by taking as a reference step 3 (Fig. 4). At approximately 825 mV a steep current increase indicates the beginning of the resonant tunneling, i.e., $\epsilon_d = \epsilon_F$. At the current onset, a sharp peak with an overshoot is observed. For higher values of bias (830–970 meV), the current rises systematically but several reproducible peaks with very small amplitudes are superimposed. Then at approximately 970 meV the tunneling process is switched off. At this bias $\epsilon_d = \epsilon_1$ where ϵ_1 is the bottom of the subband in the 2DEG (see Fig. 1).

In order to confirm that the maximum of the current observed at the end of the step (at 970 meV) is related to the switching off of the tunneling and thus corresponds to the case where the impurity level is aligned with the bottom of the 2DEG subband in the emitter, we further performed magnetotransport measurements. $I(V)$ characteristics have been measured with a magnetic field applied along the direction of the current. In Fig. 5 $I(V)$ curves between 0 and 2.4 T are plotted and the shift of the peak related to the second Landau level is clearly seen as a function of the magnetic field (the first LL is hidden in the maximum at the end of the step, but it is revealed in high magnetic fields). When $B \rightarrow 0$ T they converge to $V \approx 970$ meV, which is a clear proof that this voltage corresponds to the bottom of the subband. It means that the total width of the emitter corresponds to 140 ± 10 meV. Using the correspondence between the Landau level separation measured in $I(V)$ characteristics and the one calculated in energy scale $\hbar\omega_c$ (where ω_c is the cyclotron frequency), we were able to recalculate the width of the emitter into energy, obtaining $\epsilon_F - \epsilon_1 \approx 4.8$ meV.

Referring to Fig. 5, we would like to note that within each $I(V)$ curve a rich structure of very sharp peaks appears in magnetic field. The average separation between these peaks is of the order of 0.1 meV and they are very sensitive to the magnetic field. Similar observations have already been reported in the literature.[8] The origin of those structures is not

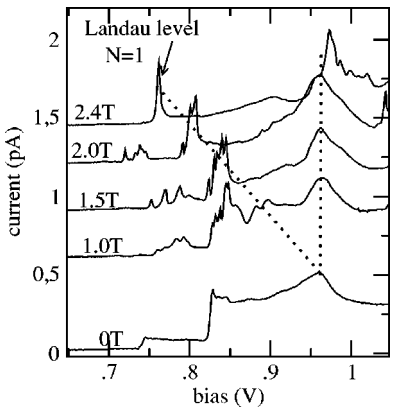

FIG. 5. $I(V)$ curves at $T=30$ mK in the presence of a magnetic field of 0, 1, 1.5, 2, and 2.4 T. The field is oriented along the direction of the current. Curves have been vertically shifted, the shift is proportional to the magnetic field. Dotted lines are guides for eyes for the second Landau level and the bottom of the conduction band.

fully understood yet and some further investigations must be performed.

When the tunneling process stops, for voltages higher than 970 meV, a smooth decrease of the tunneling current is observed. It should be noted that the current never falls to its value observed before the beginning of the tunneling, but remains at a higher level. We propose that this feature (current tail), together with the systematic rise of the current as a function of bias during the tunneling, is due to the coupling to the environment (contribution of nonresonant tunneling is negligible in this scale), which is realized by interactions with phonons.[15] This issue will be discussed in the next paragraphs, where we present our model and results of the calculations. In the last part of the paper we will focus on the fine structures observed within the steps and discuss the current maximum at Fermi energy.

V. MODEL

Tunneling transfer times have been calculated taking into account only the interactions with the GaAs longitudinal acoustic phonons. Indeed, optical phonons have much higher energy ($\geqslant$30 meV) and cannot be responsible for the observed features that appear at typical energies of only a few meV. To compute the tunneling time $\tau_{\mathbf{k}_i}$ from a 2DEG eigenstate $|\mathbf{k}_i\rangle$ to the impurity we use the Fermi golden rule

$$\frac{1}{\tau_{\mathbf{k}_i}}=\frac{2\pi}{\hbar}\sum_{\mathbf{q}}|\langle\varphi|\mathcal{H}_{\text{el-ph}}|\mathbf{k}_i\rangle|^2\delta[\epsilon_f+\hbar\omega(\mathbf{q})-\epsilon_i], \quad (1)$$

where $\mathbf{k}_i$ is the wave vector of the electron in the 2DEG plane, $\epsilon_{i(f)}$ is the energy of the initial (final) electron state and the kets $|\varphi\rangle$ and $|\mathbf{k}_i\rangle$ refer to the eigenstates of the impurity and of the 2DEG, respectively. In this equation the summation is performed over all the final states with one phonon of energy $\hbar\omega(\mathbf{q})$. Because our experiments are performed at very low temperature only phonon emission processes are relevant.

The computation of the matrix elements requires the knowledge of the wave functions. We adopt the envelope function formalism in the single parabolic band approximation.

The envelope eigenfunctions of the 2DEG are approximated by the so-called modified Fang-Howard wave function which is given by[13]

$$\langle z,\mathbf{r}|\mathbf{k}\rangle=\psi(z)\frac{1}{L}e^{i\mathbf{k}\cdot\mathbf{r}}, \quad (2)$$

where $\mathbf{r}$ and z are the projections of the electron position vector in the 2DEG plane and in the direction of the current, respectively, L is the lateral length and $\psi(z)$ is defined by

$$\psi(z)=Nz_0e^{K_bz/2} \text{ if } z\leqslant 0 \text{ (AlAs barrier)},$$

$$\psi(z)=N(z+z_0)e^{-bz/2} \text{ if } z\geqslant 0 \text{ (GaAs)}. \quad (3)$$

Here N, z_0 and b are defined by

$$b=\left[\frac{48\pi e^2m_e}{\kappa\hbar^2}\left(n_{\text{depl}}+\frac{11}{32}n_s\right)\right]^{1/3}, \quad (4)$$

$$N=\sqrt{\frac{b^3}{2}}\times\frac{1}{\sqrt{1+bz_0+\frac{1}{2}b^2z_0^2\left(1+\frac{b}{K_b}\right)}}, \quad (5)$$

$$z_0=\frac{2}{b+K_b\frac{m_e}{m_b}}, \quad (6)$$

$$K_b=2\frac{\sqrt{2m_b(\epsilon_b-\epsilon_i)}}{\hbar}, \quad (7)$$

where m_e and m_b are the electron masses in the well and in the barrier, respectively, $m_e=0.067m_0$, $m_b=0.124m_0$, κ is the dielectric constant in the well $\kappa=12.9\times\kappa_0$, n_s is the electron density of states $n_s=1.32\times10^{15}$ m^{-2}. Here, n_{depl} is the concentration of residual acceptors with a typical value of 6×10^{14} m^{-2}, m_0 is the free electron mass, and κ_0 is the dielectric constant in the vacuum, ϵ_b is the barrier height and ϵ_i is the energy of the electron.

For the sake of simplicity the wavefunction of the impurity inside the AlAs quantum well is approximated by a spherical Gaussian function

$$\langle z,\mathbf{r}|\varphi\rangle=\varphi(x)\varphi(y)\varphi(z-z_i), \quad (8)$$

where

$$\varphi(x)=\left(\frac{1}{\pi\sigma^2}\right)^{1/4}e^{-x^2/2\sigma^2}, \quad (9)$$

z_i is the position of the impurity along the growth direction and σ corresponds to the spatial extent of the donor wavefunction and is comparable to the Bohr radius of a Si impurity. In the AlAs barrier this value is estimated to be close to 2.6 nm. The adopted form of the donor wave function is a very crude approximation, which cannot give good absolute

values for the tunneling rates. However, we believe that it is good enough for the qualitative description of the physical phenomena involved.

The electron-phonon interaction is given by

$$\mathcal{H}_{\text{el-ph}}=\sum_{\mathbf{q}}\ [\alpha(q)e^{-i\mathbf{q}_{\parallel}\cdot\mathbf{r}}e^{-iq_z z}b_{\mathbf{q}}^{\dagger}+\text{H.c.}], \tag{10}$$

where $\mathbf{q}_{\parallel}$ is the phonon wave vector in plane of the 2DEG, $b_{\mathbf{q}}^{\dagger}$ is the creation operator for a phonon of wave vector $\mathbf{q}$ (in all the space directions), and $\alpha(q)$ are given either by

$$\alpha(q)=\frac{ee_{\text{pz}}^{*}}{\kappa}\sqrt{\frac{\hbar}{2\rho c_s\Omega}}\frac{1}{\sqrt{q}} \tag{11}$$

for the piezoelectric scattering or by

$$\alpha(q)=D\sqrt{\frac{\hbar}{2\rho c_s\Omega}}\sqrt{q} \tag{12}$$

for the deformation potential scattering, where D is the deformation potential constant, ρ is the GaAs density, c_s is the sound velocity in GaAs, e_{pz}^{*} is the piezoelectric constant (13 eV, 5300 kg/m^3, 3700 m/s, and 0.14 eV respectively), Ω is the volume of the crystal. We have assumed that the phonons obey the Debye's law.

The total phonon-assisted tunneling rate τ is obtained by summing over the initial states $|\mathbf{k}_i\rangle$: $\tau^{-1}=\Sigma_{\mathbf{k}_i}\tau_{\mathbf{k}_i}^{-1}$ and an usual calculation[16] gives

$$\frac{1}{\tau}=\frac{4}{\hbar}\frac{\Omega}{(2\pi)^3}\int_{k_0}^{k_F}dk_i k_i\int_0^{2\pi}d\theta\int_0^{q_D}dq_{\parallel}q_{\parallel}|f(q_z)|^2|\alpha(q)|^2 \times\left[\frac{1}{\hbar c_s}\frac{q}{q_z}\right]F^2(k_i,q_{\parallel},\theta) \tag{13}$$

where $k_0=\sqrt{2m_e\max(\epsilon_d-\epsilon_1,0)}/\hbar$, k_F is the 2DEG wave vector at the Fermi energy ϵ_F, q_D is the Debye wave vector, θ is the angle between $\mathbf{k}_i$ and $\mathbf{q}_{\parallel}$, F is given by

$$F=2\sqrt{\pi}\sigma\exp\left(-\frac{1}{2}k_i^2\sigma^2-\frac{1}{2}q_{\parallel}^2\sigma^2+k_iq_{\parallel}\sigma^2\cos\theta\right) \tag{14}$$

and $f(q_z)$ is a form factor defined by

$$f(q_z)=\int_{-\infty}^{\infty}\varphi(z)\psi(z)e^{-iq_z z}dz, \tag{15}$$

where integration can be performed over the whole space since φ and ψ are localized. Finally q_z is given by the energy conservation

$$q_z=\sqrt{\left(\frac{(\epsilon_i-\epsilon_d)}{\hbar c_s}\right)^2-q_{\parallel}^2} \tag{16}$$

and $q_z^2+q_{\parallel}^2=q^2$.

VI. RESULTS OF THE CALCULATIONS

In this section we present the numerical results. Figure 6 shows the computed phonon-assisted tunneling rates for both deformation potential and piezoelectric interactions. The rates are plotted as a function of the donor energy ϵ_d. The energy reference is the energy ϵ_1 of the bottom of the 2DEG subband. Both interactions have the same qualitative behavior, but the deformation potential interaction gives a rate one order of magnitude higher than that arising from the piezoelectric interaction. At the beginning, the rates increase with ϵ_d to reach a maximum close to $\epsilon_d=\epsilon_1$. This increase is mainly due to the fact that the number of electrons available for phonon-assisted tunneling increases when ϵ_d decreases. Finally, when ϵ_d diminishes further and goes below the 2DEG subband, the rates diminish too: the number of initial states available for tunneling remains constant but the tunneling rates with phonons of high energy are strongly reduced by the form factor $f(q_z)$ appearing in Eq. (13). This decreasing tail can be ascribed to the fact that only acoustic phonons with small $\mathbf{q}$ contribute strongly to the relaxation time in a 2DEG.

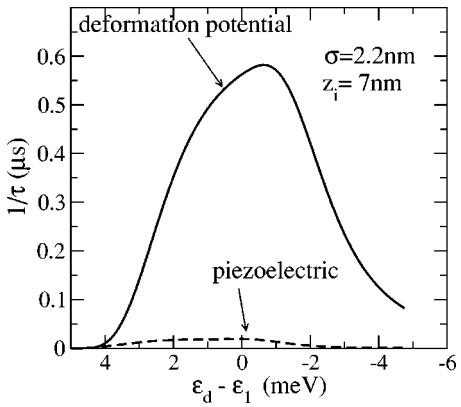

FIG. 6. Phonon-assisted tunneling rates for both deformation potential and piezoelectric interactions.

In order to describe the observed shape of the tunneling current, one should take into account not only the phonon-assisted tunneling but also the elastic one. In the sequential model of the tunneling, one should consider two processes: transfer from the emitter to the impurity and from the impurity to the collector. In our system, the donors observed at low biases are located on the collector side of the barrier (even if the change of donor binding energy at the edge of QW is taken into account[12,13]). The total current can be expressed by the tunneling rates between the emitter and the impurity only:

$$I=e\left(\frac{1}{\tau}+\frac{1}{\tau_{\text{df}}}+\frac{1}{\tau_{\text{pz}}}\right), \tag{17}$$

where τ_{df} and τ_{pz} stand for the deformation potential and the piezoelectric potential contributions, respectively, τ stands for the elastic tunneling contribution and is inversely proportional to the square of the overlap between the donor wave function and the electron wave function in the emitter.

The amplitude of elastic contribution is adjusted to fit the experimental value of the current measured just above the threshold, where the contribution of phonon-assisted currents

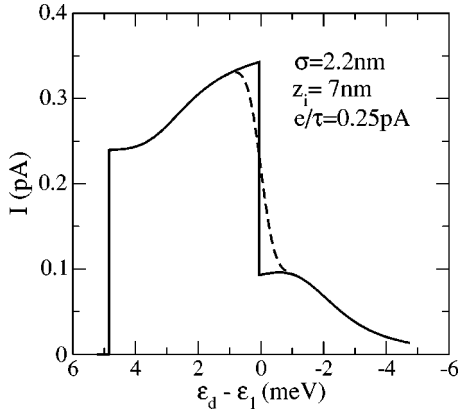

FIG. 7. Solid line: computed $I(V)$ curve taking into account the elastic tunneling contribution and both phonon-assisted contributions. Dashed line: a phenomenological broadening of the emitter density of states has been added in the calculation.

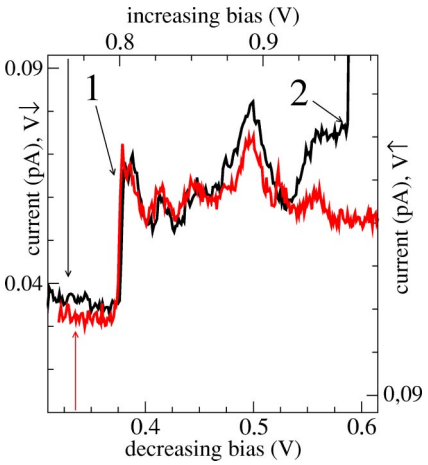

FIG. 8. First $I(V)$ step for both increasing and decreasing biases.

is still negligible and singularity at ϵ_F already vanishes. If we take a donor placed close to the collector side of the barrier, e.g., $z_i = 7-9$ nm, we get a reasonable agreement with the experiment for $\sigma = 2.2-3.2$ nm, respectively. The values of σ are of the same order of magnitude as the Si Bohr radius. The result of the calculation for $z_i = 7$ nm and $\sigma = 2.2$ nm is presented in Fig. 7 with a solid line. The calculated current rises up to $\epsilon_d = \epsilon_1$, in agreement with the experiment and the current tails at higher bias are reproduced. The calculated sharp decrease of the current at $\epsilon_d = \epsilon_1$ is related to the steplike DOS in the emitter which is reflected in the elastic contribution.

In order to improve the agreement with the experiment one has to find the reason why the elastic contribution does not change so abruptly at $\epsilon_d = \epsilon_1$. This can happen due to, e.g., the disorder-related broadening of the DOS. Indeed, in the magnetic field results (see Fig. 5)—Landau level $N = 0$ is always considerably broadened, almost independently of magnetic field. Possibly there is a band tail at the bottom of the conduction band induced by disorder. We can take it into account by including in our model the convolution of the unperturbed DOS with a Gaussian. The result is shown in Fig. 7 with a dashed line. The FWHM of the Gaussian was taken to be 0.8 meV. One can also expect that more exact many-body calculations of the current would lead to such a broadening.[17] Indeed, the Fermi golden rule is an approximation that does not take into account tunneling events with more than one phonon.

VII. THE FINE STRUCTURES

Finally, we want to comment on the detailed structures observed on the steps, which have not been discussed until now. The first striking feature is the sharp maximum at the current onset, i.e., at the Fermi energy, see Fig. 4. This maximum is due to the Coulomb interaction between electrons in the 2DEG and the impurity state. This effect, known in x-ray spectroscopy, was first predicted for the case of tunneling through a localized level by Matveev and Larkin.[18] First experimental confirmations were presented by Geim *et al.*,[19] who performed careful temperature analysis in order to demonstrate a singular behavior of the current at the Fermi energy. In our case the system changes its properties due to charging effects during voltage sweep. Instead of overcoming these effects, we take advantage of them. In the $I(V)$ curves a hysteresis of the tunneling current is observed: by sweeping up and down the bias, the same structures are observed in different bias ranges and they have different widths in the voltage scale. However, by applying a linear transformation to the bias and a vertical shift to the current (the need for the latter is related to charging of some capacitance during the voltage sweep), it is possible to superimpose the two $I(V)$ curves for both directions of bias sweep. This is shown in Figs. 8 and 9 where the different axes are labeled for both bias directions. One clearly sees that the main difference is a shift of the current onset at the Fermi level in Fig. 9. It means that the number of electrons in the emitter was slightly modified. But no matter what the position of the onset was, the observed maximum remains stuck to the Fermi level.

Following Refs. 18 and 19, the Fermi edge singularity has a power-law shape of the form

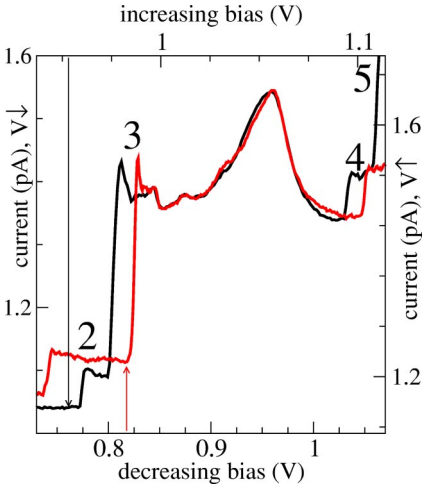

FIG. 9. Third $I(V)$ step for both increasing and decreasing biases.

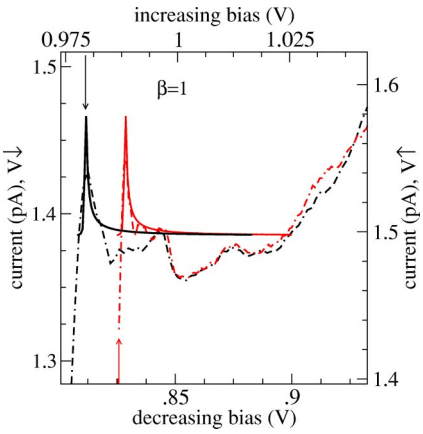

FIG. 10. $I(V)$ curves for both increasing and decreasing biases, best fit obtained with $\beta \approx 1$, $\Gamma_c \approx 0.01$ meV.

$$I \propto (\sqrt{(\epsilon_F - \epsilon)^2 + \Gamma_c^2})^{-\beta} \times \left(\frac{\pi}{2} + \arctan \frac{\epsilon_F - \epsilon}{\Gamma_c} \right) \theta(\epsilon_F - \epsilon), \tag{18}$$

where ϵ is the energy of the tunneling electron, $\hbar/\Gamma_c$ is the time an electron can stay in the impurity state before escaping into the collector side and

$$\beta = \frac{3}{4\pi} (k_F d)^{-1}, \tag{19}$$

where d is the average distance between the 2DEG and the impurity state and k_F is the wave vector at the Fermi energy. In Fig. 10 we present an enlargement of step 3 from Fig. 9 for two polarizations. Despite the shift at lower biases, the two curves start to be very similar at biases higher than 0.85 V (in the lower scale of Fig. 10). It means that at biases higher than 0.85 V the many-body contribution becomes negligible and the measured current is due to noninteracting electrons only. The amplitude of this current does not depend on the bias sweep direction. This limits the range of acceptable values of fitting parameters. The voltage corresponding of ϵ_F was taken from the experimental results and the value of $k_F = 9.3 \times 10^7$ m^{-1} was calculated from the measured $\epsilon_F - \epsilon_1$. Three parameters were fitted, as in Ref. 19: the amplitude of the many-body current in Eq. (18), Γ_c and β. The best fit was obtained for $\Gamma_c \approx 0.01$ meV and $\beta \approx 1$. The average distance d evaluated from Eq. (19) is close to 2.5 nm, which is only about 4 times smaller than expected for impurity placed at the collector side of the barrier and gives a reasonable order of magnitude. The transfer time τ is of the order of 100 ps.

Another interesting feature that is worth pointing out is the existence of the hardly resolved peaks within the plateau, in Fig. 9, between 0.83 and 0.94 V (in the lower scale). We attribute them to local fluctuations of the DOS in the vicinity of an impurity.[20,21] Naturally, we can expect that if the fluctuations are different for some steps, then these steps are most probably related to different impurities and do not correspond to ground or excited states belonging to the same impurity. If we compare step 1 (Fig. 8) and step 3 (Fig. 9), we see that the detailed characteristics are different, even if the signal is much more noisy in step 1, as the values of current are very small. Thus we argue that we do really observe fluctuations of LDOS and that step 1 and 3 correspond to two different impurities.

VIII. CONCLUSION

We have studied resonant tunneling from a 2DEG through the single impurity state. We see contributions from individual impurities—each of them appears to be different from the expected rectangular shape. In particular, there is a current enhancement when the energy of the impurity approaches the energy of the bottom of the subband. If the impurity energy decreases further, the current decreases but does not vanish. We argue that this phenomenon is due to phonon-assisted tunneling processes. Other additional features like Fermi edge singularities and fluctuations of the density of states are clearly resolved. We present an original analysis which unambiguously demonstrates that the peak at the Fermi level is related to the Fermi edge singularity and not to the fluctuations of the density of states.

ACKNOWLEDGMENTS

We are indebted to X. Lafosse and L. Couraud for technical support and to L. Ferlazzo for the reactive Ion etching. This work has been partly supported by the Ministry of Scientific Research and Information Technology (Poland, Grant No. 2 PO3B 068 24), by the Région Ile de France (SESAME Project No. 1377), and by the Conseil Général de l'Essonne.

[1] R. Beresford, L. F. Luo, W. I. Wang, and E. E. Mendez, Appl. Phys. Lett. **55**, 1555 (1989).
[2] R. Teissier, J. J. Finley, M. S. Skolnick, J. W. Cockburn, J.-L. Pelouard, R. Grey, G. Hill, M. A. Pate, and R. Planel, Phys. Rev. B **54**, R8329 (1996).
[3] J. J. Finley, R. J. Teissier, M. S. Skolnick, J. W. Cockburn, G. A. Roberts, R. Grey, G. Hill, M. A. Pate, and R. Planel, Phys. Rev. B **58**, 10619 (1998).
[4] I. E. Itskevich, L. Eaves, P. C. Main, M. Henini, and G. Hill, Phys. Rev. B **57**, 7214 (1998).
[5] S. A. Vitusevich, A. Förster, K. M. Indlekofer, H. Lüth, A. E. Belyaev, B. A. Glavin, and R. V. Konakova, Phys. Rev. B **61**, 10898 (2000).
[6] M. Gryglas, J. Przybytek, M. Baj, M. Henini, and L. Eaves, High Press. Res. **18**, 63 (2000).
[7] Yu. N. Khanin, E. E. Vdovin, Yu. V. Dubrovskii, K. S. Novoselov, S.-B. Carlsson, and P. Omling, Phys. Rev. B **66**, 073302 (2002).
[8] P. C. Main, A. Thornton, R. J. A. Hill, S. T. Stoddart, T. Ihn, L. Eaves, K. A. Benedict, and M. Henini, Phys. Rev. Lett. **84**, 729 (2000).
[9] E. Lind, B. Gustafson, I. Pietzonka, and L. E. Wernersson, Phys. Rev. B **68**, 033312 (2003).

[10] M. W. Dellow, P. H. Beton, C. J. G. M. Langerak, T. J. Foster, P. C. Main, L. Eaves, M. Henini, S. P. Beaumont, and C. D. W. Wilkinson, Phys. Rev. Lett. **68**, 1754 (1992).
[11] M. Gryglas, M. Baj, B. Jouault, G. Faini, and A. Cavanna, Physica E (Amsterdam) **17**, 303 (2003).
[12] C. Mailhiot, Y.-C. Chang, and T. C. McGill, Phys. Rev. B **26**, 4449 (1982).
[13] G. Bastard, *Wave Mechanics Applied to Semiconductor Heterostructures* (Les éditions de Physique, Les Ulis, 1988).
[14] J. López-Gondar, J. d'Albuquerque e Castro, and L. E. Oliveira, Phys. Rev. B **42**, 7069 (1990).
[15] T. Fujisawa, W. G. van der Wiel, and L. P. Kouwenhoven, Physica E (Amsterdam) **7**, 413 (2000); T. Fujisawa, T. H. Oosterkamp, W. G. van der Wiel, B. W. Broer, R. Aguado, S. Tarucha, and L. Kouwenhoven, Science **282**, 932 (1998).
[16] R. Ferreira and G. Bastard, Phys. Rev. B **40**, 1074 (1989); S. Khan-ngern, I. A. Larkin, Phys. Lett. A **266**, 209 (2000).
[17] M.-H. Devoret, D. Esteve, H. Grabert, G.-L. Ingold, H. Pothier, and C. Urbina, Phys. Rev. Lett. **64**, 1824 (1990); M. Jonson, Phys. Rev. B **39**, 5924 (1989); J. König, J. Schmid, H. Schoeller, and G. Schön, *ibid.* **54**, 16820 (1996).
[18] K. A. Matveev and A. I. Larkin, Phys. Rev. B **46**, 15337 (1992).
[19] A. K. Geim, P. C. Main, N. La Scala, Jr., L. Eaves, T. J. Foster, P. H. Beton, J. W. Sakai, F. W. Sheard, M. Henini, G. Hill, and M. A. Pate, Phys. Rev. Lett. **72**, 2061 (1994).
[20] I. V. Lerner and M. E. Raikh, Phys. Rev. B **45**, 14036 (1992).
[21] T. Schmidt, R. J. Haug, V. I. Fal'ko, K. v. Klitzing, A. Förster, and H. Lüth, Europhys. Lett. **36**, 61 (1996).